1999176551

EFFECT OF SWIRL ON NOISE FROM A HIGH ASPECT RATIO RECTANGULAR NOZZLE

M.K. Ponton, J.M. Seiner, and L.K. Mitchell
NASA Langley Research Center
Hampton, Virginia

524-07

409532
16P.

INTRODUCTION

Based on extensive work performed by Dr. Thomas H. Sobota (Advanced Projects Research Incorporated (APRI)) on swirling flows in circular-to-rectangular transition sections, a model assembly was designed and fabricated in support of a Phase I Small Business Innovation Research Contract between the NASA-Langley Research Center and APRI. This assembly was acoustically tested as part of this Phase I effort, the goal being to determine whether the controlled introduction of axial vorticity could affect the various noise generation mechanisms present in an underexpanded supersonic rectangular jet.

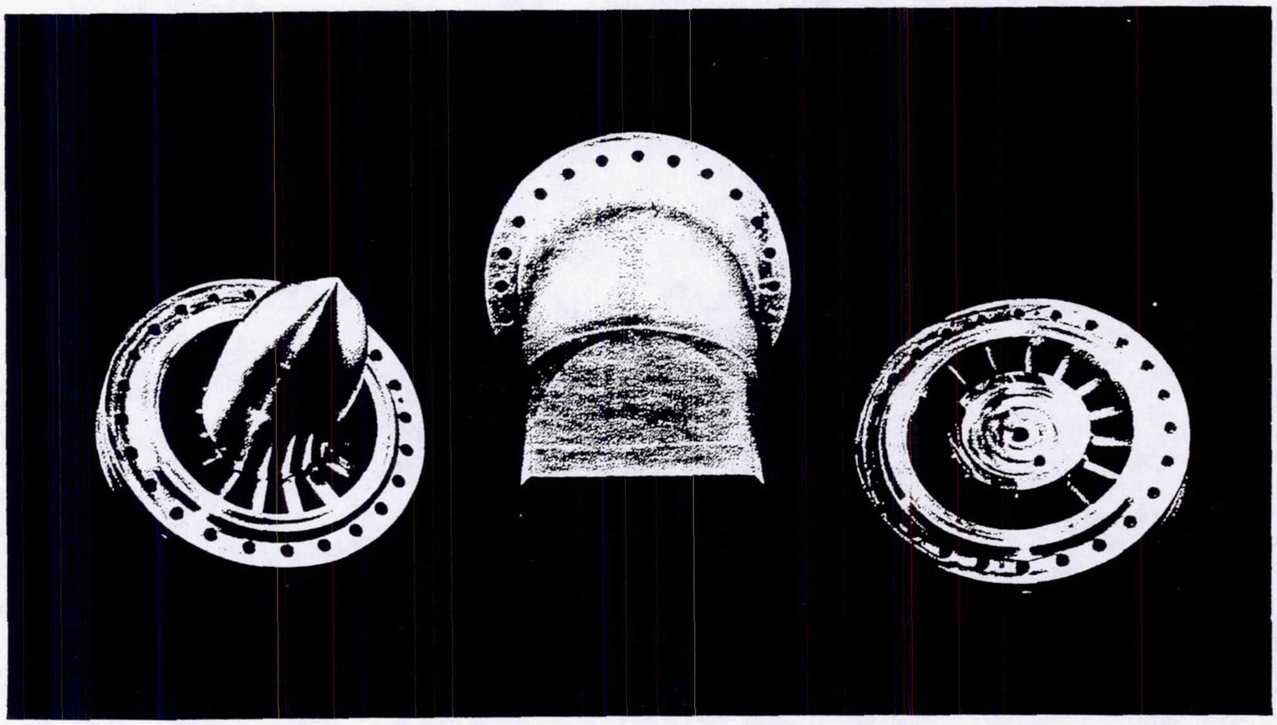

Figure 1: **TEST ARTICLE DEFINITION**

Figure 1 presents the nozzle hardware tested in this investigation. In the center of the figure is the convergent rectangular nozzle of aspect ratio 5 (exit dimensions: 1.020 in. by 5.100 in.). Three turning vane assemblies were fabricated, each containing sixteen symmetric airfoils at a fixed angle to the nozzle axis. The three turning vane angles used were 0, 15, and 30 degrees. Pictured in the left of the figure is the 30 degree swirl stage connected to the centerbody assembly. The upstream side of the centerbody is hemispherical and the downstream side is conical. The design philosophy of the centerbody and the internal contour of the nozzle assembly (i.e., the assembly which transitions from the round inlet to the rectangular exit) was such that when the centerbody is inserted into the nozzle, the internal area decreases smoothly from inlet to exit. Pictured to the right of the nozzle is the 15 degree turning vane subassembly. All hardware was fabricated from 6061-T6 aluminum alloy.

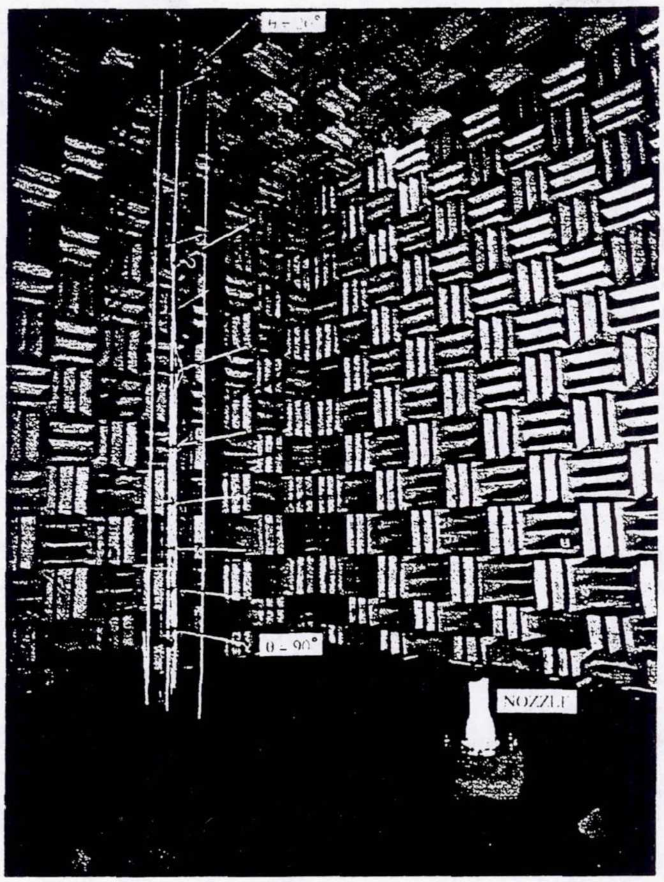

Figure 2: **EXPERIMENTAL SETUP**

The acoustic experiment was performed in the Langley Anechoic Noise Facility (LANF). This facility's interior dimensions within the wedge tips are 27.5 by 27 by 24 ft high. The LANF is capable of supplying continuous dry unheated air. Electronically controlled valves maintained the nozzle pressure ratio to within 0.5 percent of the desired set point. All pressure transducers used in the flow control system received daily calibration.

Spectra were acquired via a linear microphone (Fig. 2) array located parallel to the jet axis at a radial distance of 85.7 inches. Eight microphones were located at polar angles (θ) from 20 to 90 degrees at equal intervals of 10 degrees (the polar angle is referenced to the downstream jet axis from the nozzle exit; in Fig. 2, only the 20 and 90 degree microphones are labeled). The sensors used were 1/4-inch free-field microphones. No protective grid cap was used during data acquisition. The acoustic signals were filtered (63 Hz to 100 Khz), amplified and then multiplexed whereby spectra were then computed using a spectrum analyzer. The spectra were recorded from 50 Hz to 40 Khz using 128 spectral averages (filter bandwidth = 50 Hz). The overall voltage levels (bandlimited 63 Hz to 100 kHz) were measured with a digital RMS voltmeter which performed 256 samples per reading.

Narrowband spectra were gathered for 8 azimuthal angles (ϕ = 0, 15, 30, 45, 60, 75, 90, 135 degrees) where the azimuthal angle is referenced from the minor axis of the rectangular nozzle. Four nozzle pressure ratios were measured (1.69, 3.0, 3.5, 4.0) for the three swirl angles tested (0, 15, and 30 degrees).

Due to the magnitude of the acoustic measurements, select conditions are presented. All data presented are corrected to a circular arc of radius 85.7 inches by assuming spherical spreading. This correction is performed so that peak acoustic amplitude radiation angles can be determined.

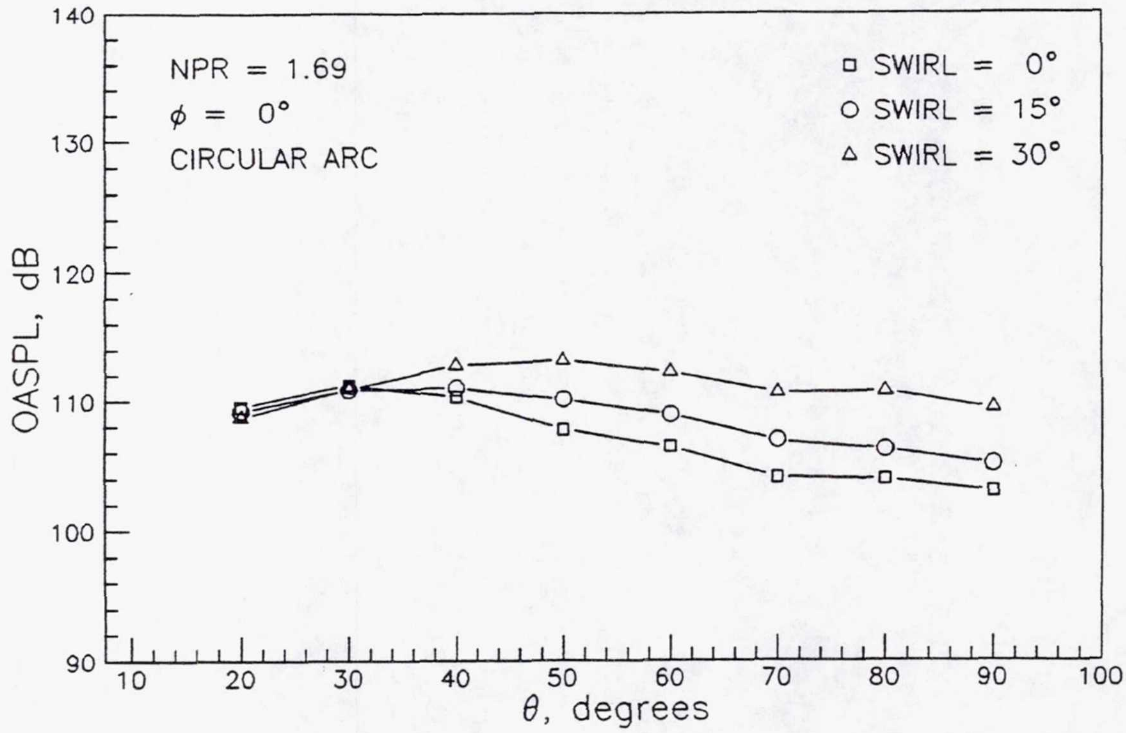

Figure 3: **OVERALL SOUND PRESSURE LEVEL (NPR = 1.69, Φ = 0 DEGREES)**

For the subsonic condition tested, Figure 3 shows that an increase in jet swirl increases the overall sound pressure level, the exceptions being at low polar angles. The low polar angles represent the peak jet noise direction which is determined by examining the direction of the maximum acoustic amplitude associated with the peak jet noise Strouhal number.

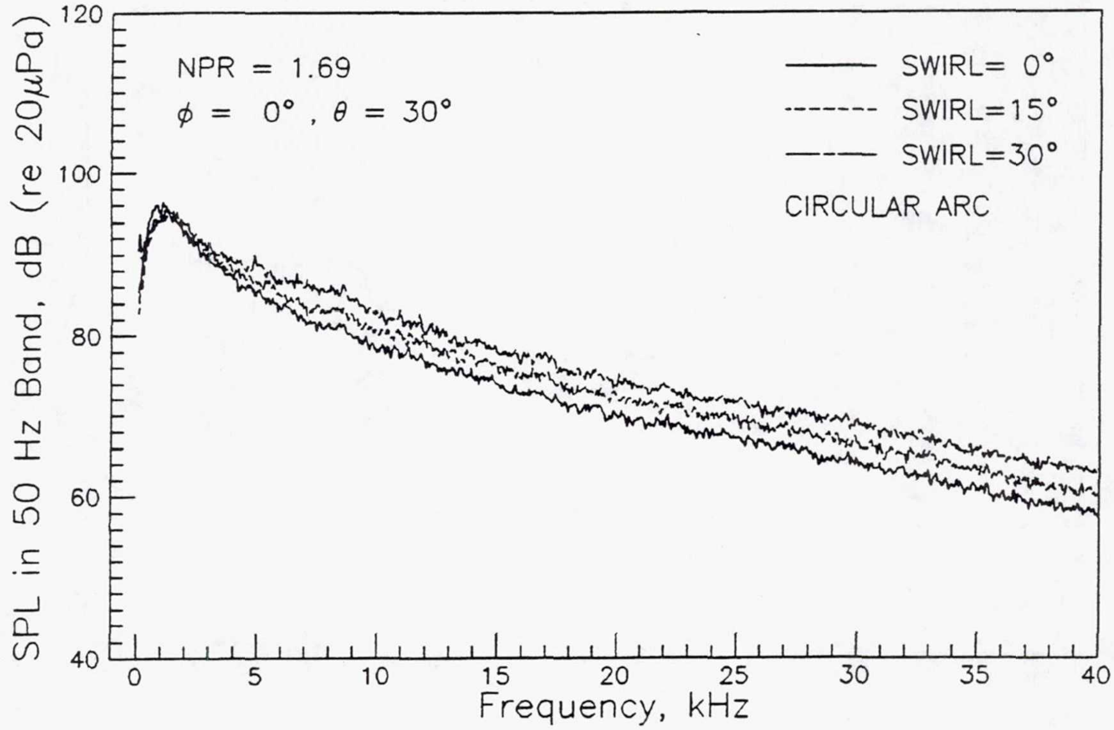

Figure 4: **NARROWBAND SPECTRA (NPR = 1.69, Φ = 0 DEG., Θ = 30 DEG.)**

The peak jet noise components can be seen in Figure 5 centered at approximately 1 kHz (the maximum jet noise amplitude for the no swirl case occurred at the measured polar angle of 20 degrees). Although the OASPL at polar angles of 20 and 30 degrees for 0 degree azimuthal angle is invariant with swirl angle (Fig. 3), Figure 4 indicates a slight decrease in the amplitude of the low frequency peak jet noise component while a broadband increase occurs for the higher frequencies when swirl is introduced.

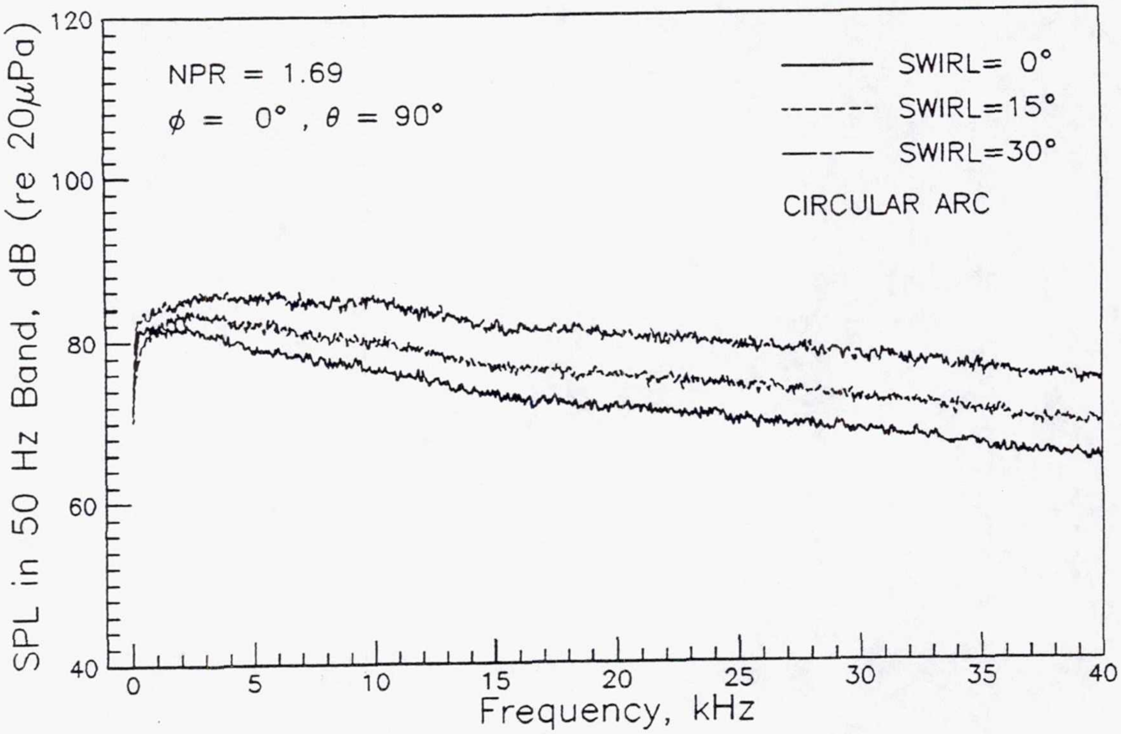

Figure 5: **NARROWBAND SPECTRA (NPR=1.69, Φ=0 DEG., Θ=90 DEG.)**

The broadband increase seen in Figure 4 is also evident at other polar angles of which Figure 5 is representative. Similar peak jet noise reductions and high frequency increases are seen for the other azimuthal angles tested. These high frequency increases may be an indicator that the addition of axial vorticity has increased the amplitude of the high frequency sources located near the nozzle exit. It is at this location that the dominant portion of high frequency noise is generated.

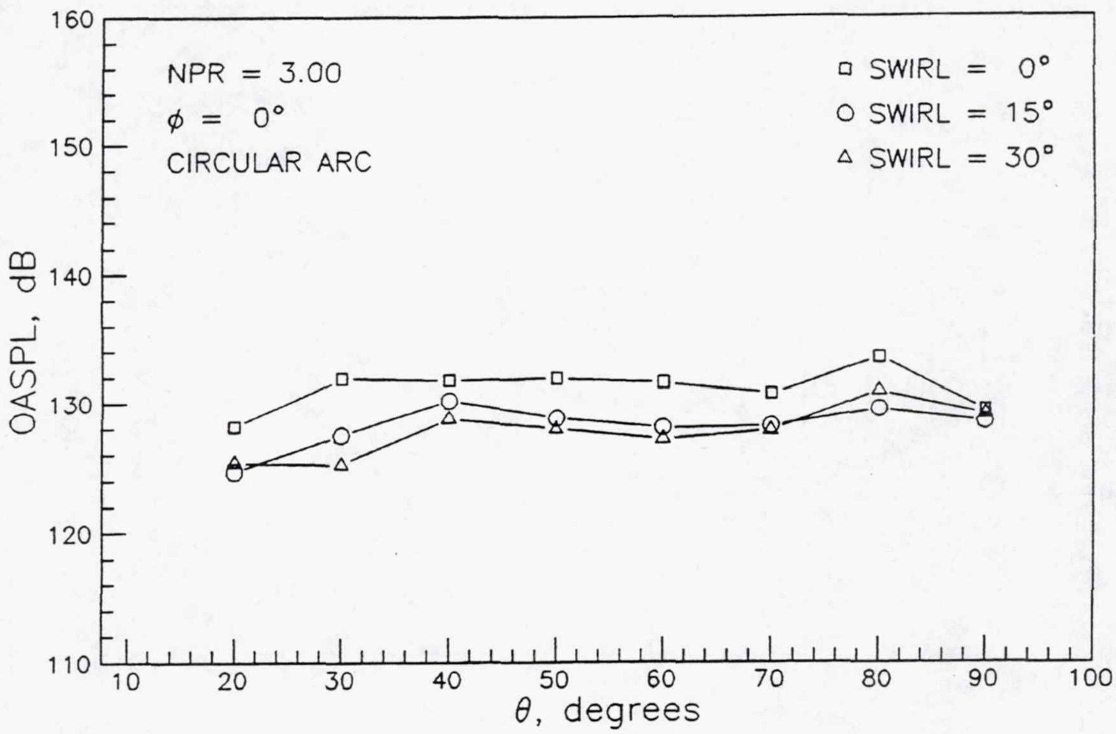

Figure 6: **OVERALL SOUND PRESSURE LEVELS (NPR=3.00, Φ=0 DEG.)**

The overall sound pressure level data (Fig. 6) indicate that an increase in jet swirl can provide noise reduction for supersonic operating conditions. Although not shown, for higher azimuthal angles the OASPL benefit occurs only at low polar angles.

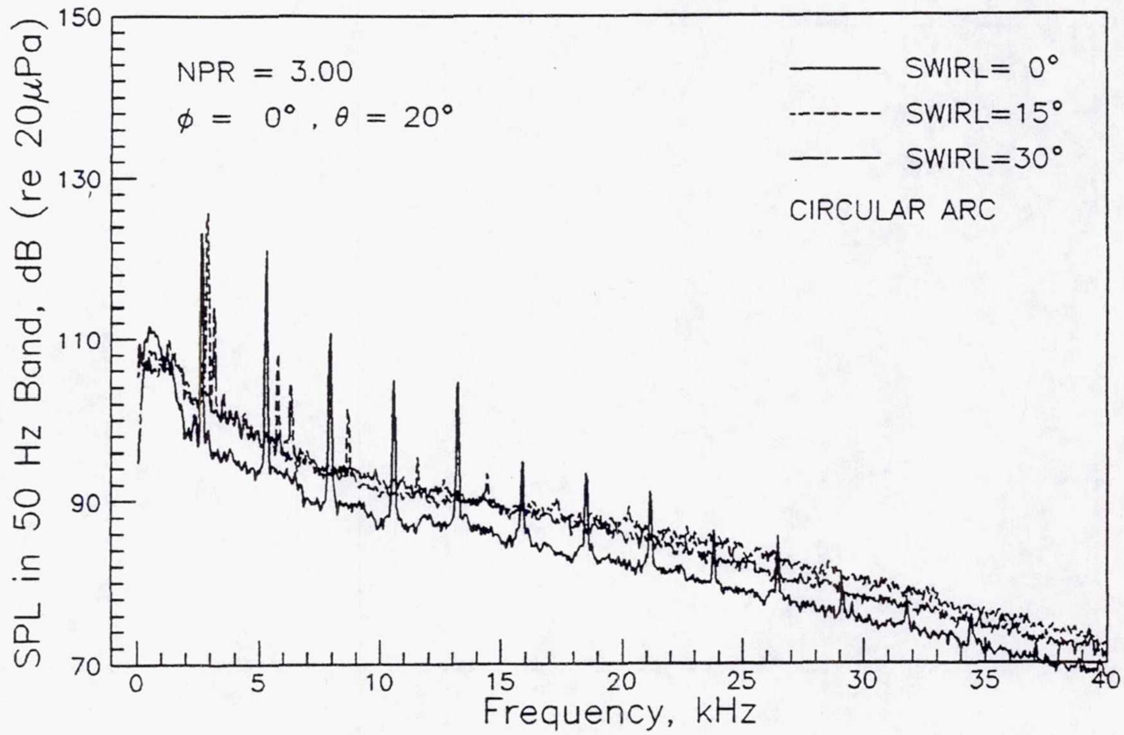

Figure 7: **NARROWBAND SPECTRA (NPR=3.00, Φ=0 DEG., Θ=20 DEG.)**

Figure 7 indicates that swirl reduces the low frequency jet noise amplitude seen at approximately 1 kHz (this is more evident in the peak jet noise direction of $\theta=30$ degrees presented in Fig. 8). Note that swirl has increased the frequency of the screech fundamental (located between 2 and 3 kHz). The amplitude of the screech harmonics have significantly decreased with increasing swirl (true for most polar angles). Except for the low frequency jet noise peak, increasing swirl increases the broadband spectrum level. The difference in the spectrum levels of the 15 and 30 degree swirl angles is small below 20 kHz.

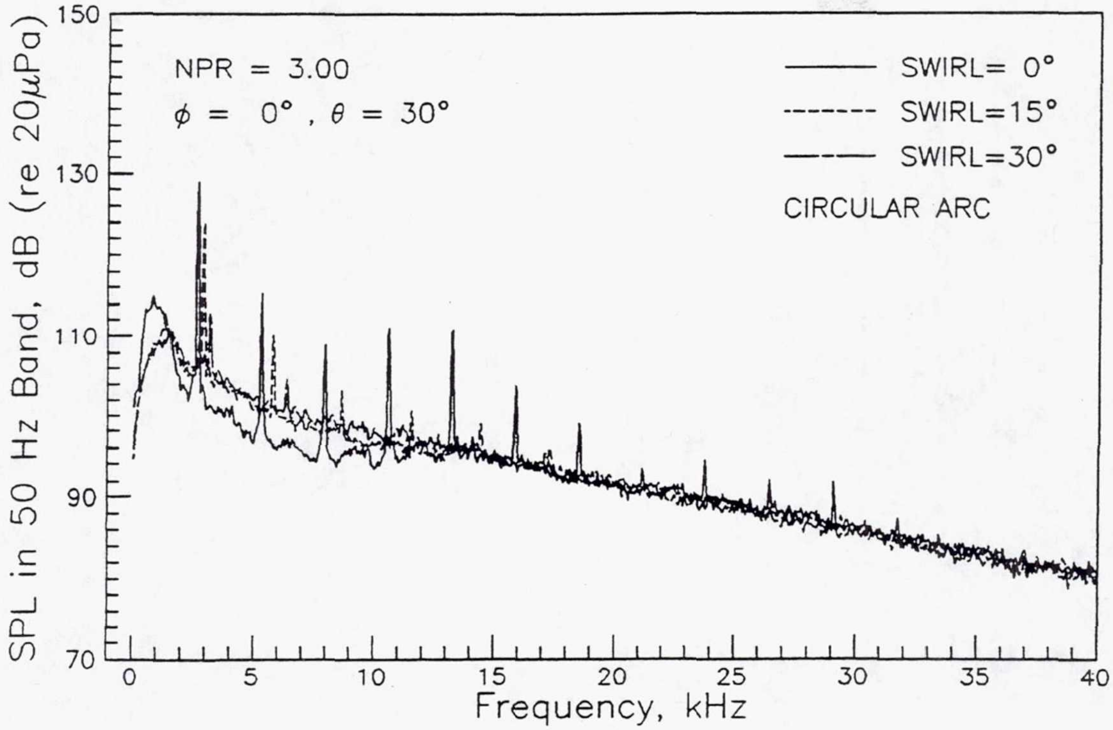

Figure 8: **NARROWBAND SPECTRA (NPR=3.00, Φ=0 DEG., Θ=30 DEG.)**

At a polar angle of 30 degrees (Fig. 8), the spectral shape for the baseline configuration (0 degree swirl) has changed where the amplitude above about 9 kHz has increased to closely match the swirling configurations. As the polar angle increases, the spectral shape of the no swirl case begins to match that of the swirling flows. The high frequency amplitude also begins to increase with swirl as the polar angle approaches 90 degrees.

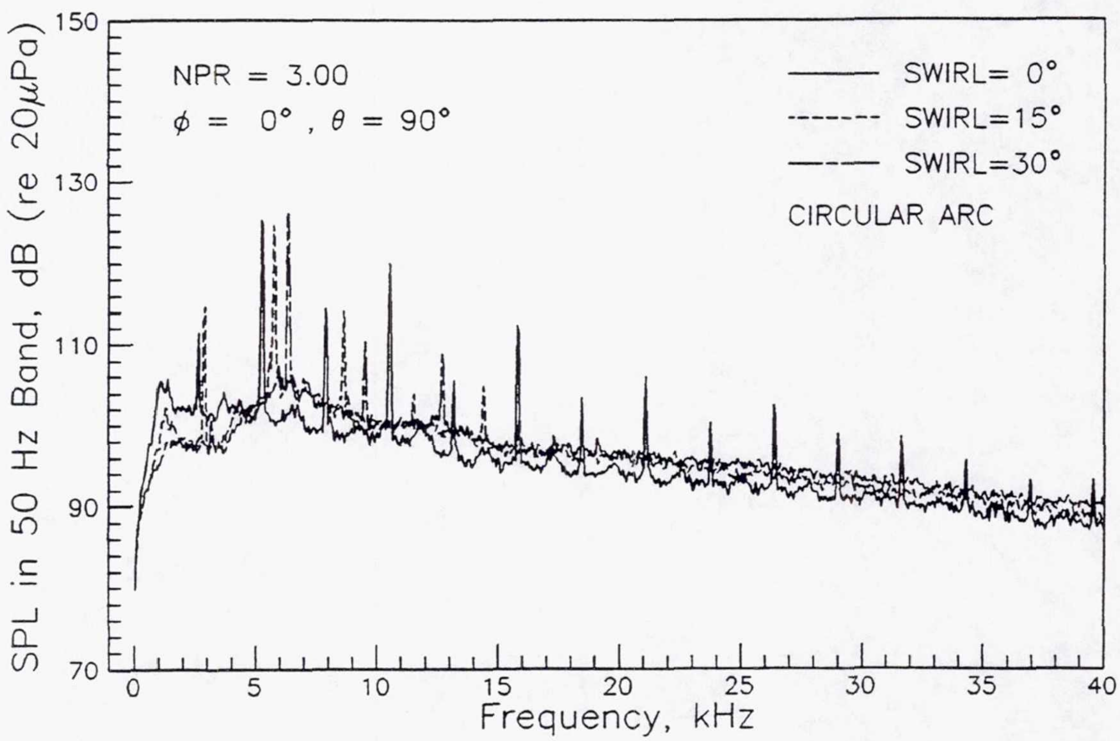

Figure 9: **NARROWBAND SPECTRA (NPR=3.00, Φ=0 DEG., Θ=90 DEG.)**

Figure 9 shows that while the low frequency reductions seen at the low polar angles are still present (approximately 1 kHz), the addition of swirl has increased not only the spectrum level at high frequencies but also the broadband shock associated noise at approximately 6.5 kHz. The affect of swirl on the amplitude of the second and third screech harmonics is minimal while the amplitude of higher harmonics is still reduced.

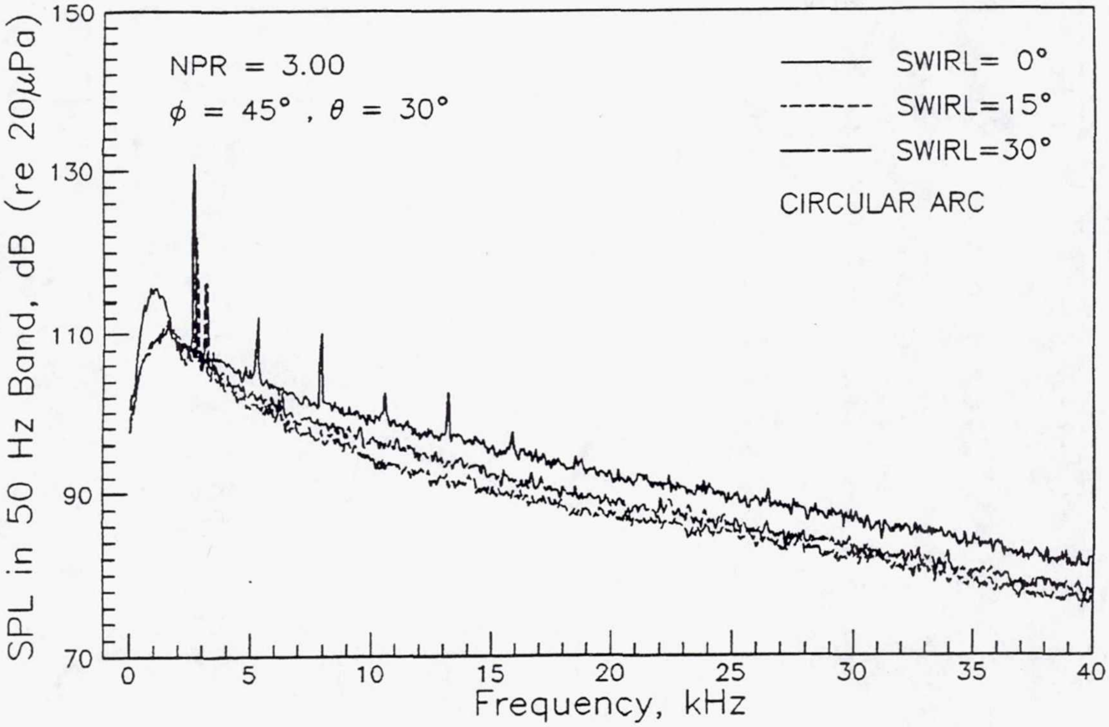

Figure 10: **NARROWBAND SPECTRA (NPR=3.00, Φ= 45 DEG., Θ=30 DEG.)**

At an azimuthal angle of 45 degrees, Fig. 10 indicates that the high frequency amplitude decreases for increasing swirl. This effect is true only for low polar angles. Similar to the $\phi=0$ degree condition, the amplitude of the screech fundamental and its harmonics is reduced by swirl addition. Also for the azimuthal angle of 45 degrees, the low frequency jet noise amplitude is reduced by introducing axial vorticity as can be seen in the broadband component located at 1 kHz.

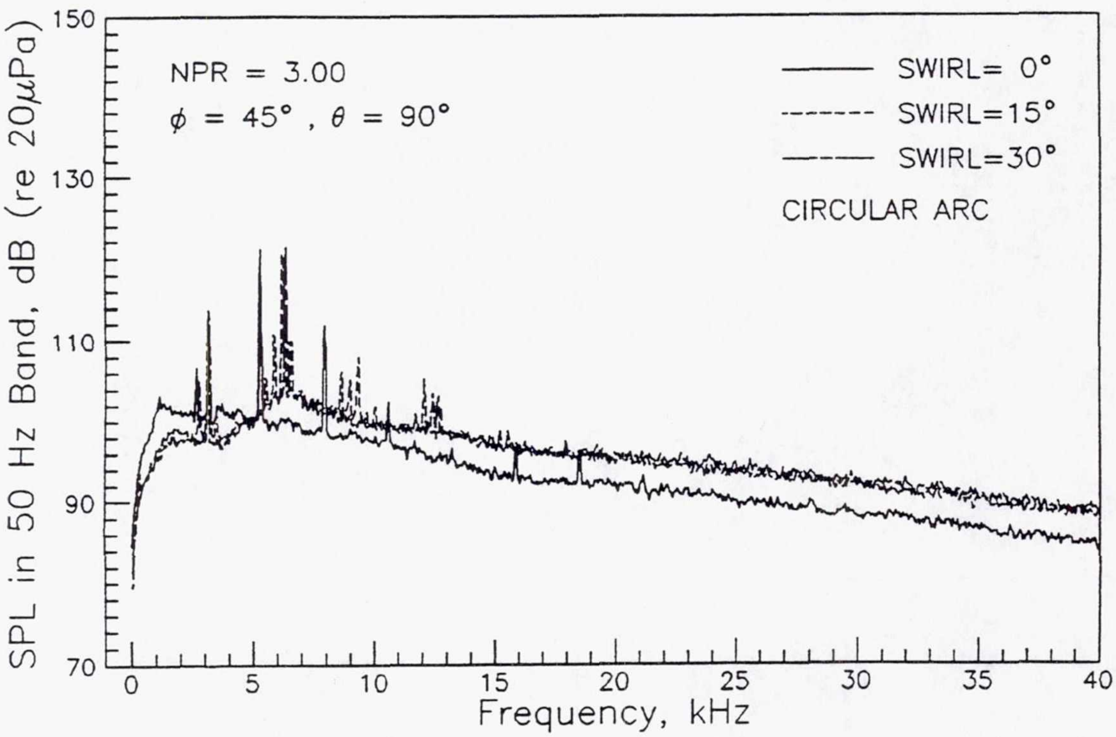

Figure 11: **NARROWBAND SPECTRA (NPR=3.00, Φ=45 DEG., Θ=90 DEG.)**

The acoustic effects of swirl addition at Phi=45 degrees (Fig. 11) is similar to those at $\phi=0$ degrees (fig. 9) for the normal polar angle. These effects are: low frequency jet noise reduction, increase in broadband hock noise, increase in the high frequency spectrum level, minimal affect on the second (and for the 15 degree swirl case third) screech harmonic amplitude. Also note that at the emission angle of Fig. 11, the addition of swirl has created additional narrowband peaks to occur in the spectrum which can be seen near the screech harmonics.

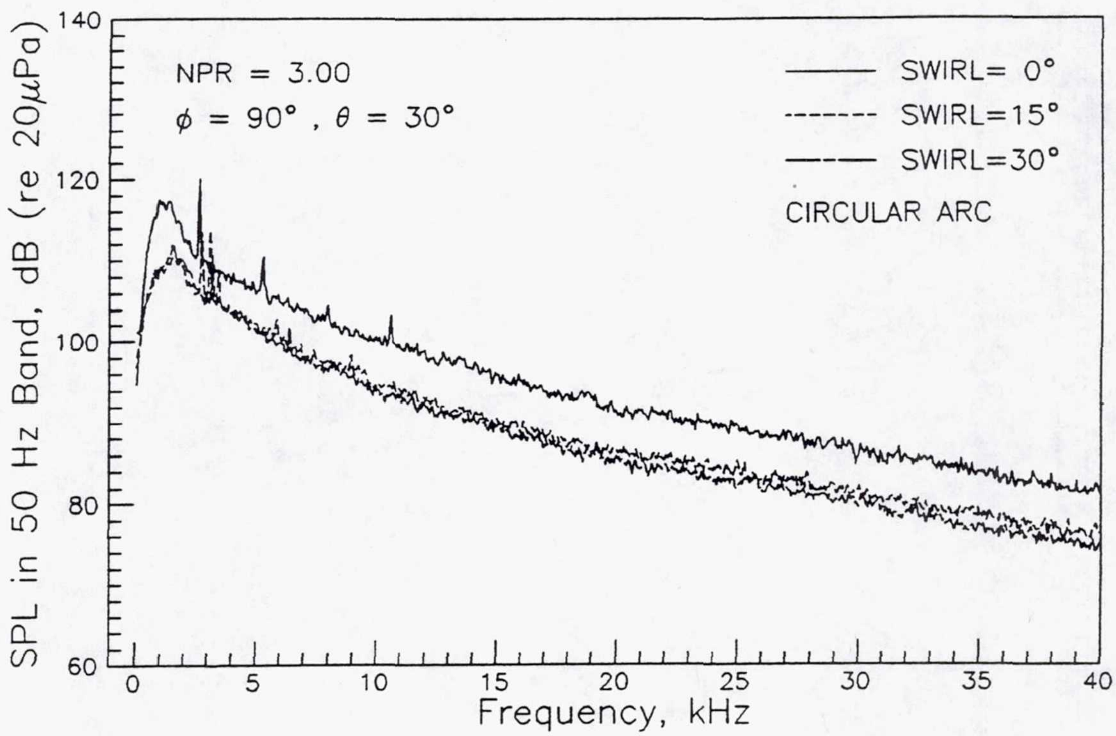

Fig. 12: **NARROWBAND SPECTRA (NPR=3.00, Φ=90 DEG., Θ=30 DEG.)**

Figure 12 represents data measured along the major axis of the nozzle (i.e., in a direction normal to the plane containing the minor axis and the nozzle centerline). Broadband amplitude decreases are evident when swirl is introduced into the flowfield. Note that for the baseline condition (0 degree swirl) screech emission is not large in this radiation direction. The spectral differences between the 15 and 30 degree swirl configurations are minimal in this figure.

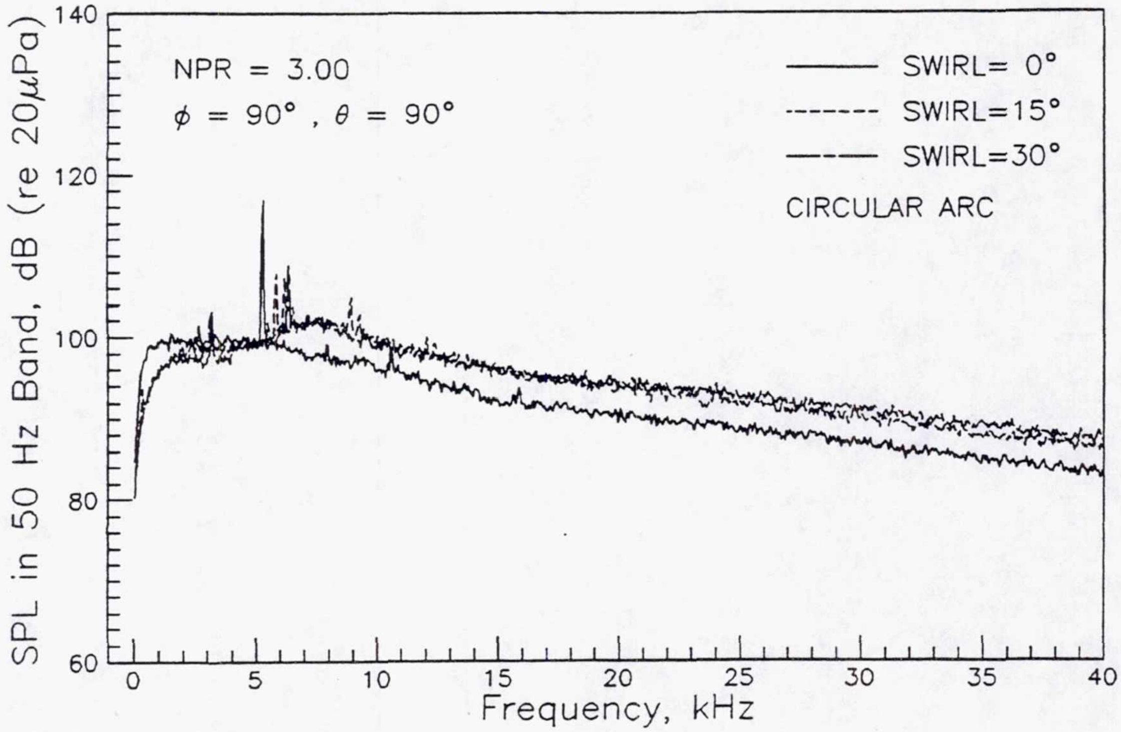

Figure 13: **NARROWBAND SPECTRA (NPR=3.00, Φ=90 DEG., Θ=90 DEG.)**

Figure 13 indicates that the effects seen by swirl addition in Figures 9 and 11 (ϕ=0 and 45 degrees, respectively) are still present at ϕ=90 degrees except that the second harmonic amplitude is no longer similar between the no swirl and swirl conditions.

CONCLUSIONS

Introducing axial vorticity in the manner of this research program has been observed to cause:

- Broadband high frequency increase (NPR = 1.69)
- Peak low frequency jet noise reduction
- Broadband shock noise increase (supercritical NPR's)
- Screech harmonic reduction (NPR = 3.0, 3.5)